frontiers in Marine Science

TYPE Original Research
PUBLISHED 15 July 2026
DOI 10.3389/fmars.2026.1873334

Check for updates

OPEN ACCESS

EDITED BY
Xinchen Gu,
South China University of Technology,
China

REVIEWED BY
Nurfadillah,
Syiah Kuala University, Indonesia
Ömer Akgüller,
Muğla Sıtkı Koçman University, Türkiye

*CORRESPONDENCE
Luis Alberiko Gil-Alana
alana@unav.es

RECEIVED 05 May 2026
REVISED 10 June 2026
ACCEPTED 16 June 2026
PUBLISHED 15 July 2026

CITATION
Caporale GM, Gil-Alana LA, Carmona-González N and Romero-Rojo MF (2026) Trends and persistence in ocean acidification as measured by station ALOHA. *Front. Mar. Sci.* 13:1873334. doi: 10.3389/fmars.2026.1873334

Trends and persistence in ocean acidification as measured by station ALOHA

Guglielmo Maria Caporale[1], Luis Alberiko Gil-Alana[2,3]*, Nieves Carmona-González[3] and Maria Fatima Romero-Rojo[3]

[1]Department of Economics and Finance, Brunel University London, London, United Kingdom, [2]Faculty of Economics, and NCID, University of Navarra, Pamplona, Spain, [3]Facultad de Derecho, Empresa y Gobierno, Universidad Francisco de Vitoria, Pozuelo de Alarcón, Spain

Ocean acidification, largely driven by the uptake of anthropogenic carbon dioxide, is reflected in a sustained decline in seawater pH. This paper examines the dynamics of surface-ocean pH at Station ALOHA over the period 1985–2024 using fractional integration methods, which allow for a flexible characterisation of persistence and trend behaviour. The differencing parameter is estimated under alternative assumptions concerning the error term, namely white-noise and autocorrelated Bloomfield disturbances, and recursive estimation is used to assess the evolution of the relevant parameters over time. The results show a negative and statistically significant time trend in both the original and logged pH series. The estimates of the differencing parameter are positive and significantly different from zero in all cases, providing evidence of long-memory behaviour. Under white-noise errors, the estimate of the differencing parameter is 0.89 and the unit-root hypothesis cannot be rejected, whereas allowing for autocorrelation yields an estimate of approximately 0.55, implying mean reversion with long-lasting but transitory effects of shocks. Recursive estimates further indicate that both persistence and the magnitude of the negative pH trend have increased over time. These findings suggest that pH dynamics at Station ALOHA are characterised by a persistent decline and slow adjustment following disturbances, highlighting the importance of long-term ocean monitoring and modelling approaches that account for fractional dependence. Nevertheless, the results should be interpreted with caution because the analysis is based on a single long-term record combining observational and reconstructed data.

KEYWORDS
fractional integration, ocean acidification, persistence, PH level, recursive estimation, station ALOHA

1 Introduction

Ocean acidification, defined as a sustained decrease in surface water pH due largely to the absorption of anthropogenic carbon dioxide (CO_2), is one of the most apparent chemical consequences of human activities for the ocean-atmosphere system (Friedlingstein et al., 2025; Jiang et al., 2023; Steiner and Reader, 2024; Vasanth et al., 2025). It is worth noting that pH is measured on a logarithmic scale, so small changes in pH values can have big chemical significance. The seriousness of this problem is such that the UN has felt the need to specify a Sustainable Development Goal to address it (14.3, "Minimize and address the impacts of ocean acidification, including through increased scientific cooperation at all levels"). Long-term observations of seawater pH have become a key indicator for assessing the chemical state of the ocean (United Nations, 2025; Global Goals, 2023). Acidification represents one of the main threats to marine ecosystems; therefore, analyzing the properties of pH time series and their degree of persistence allows for the identification of trends and the assessment of acidification's impact on the climate. Knowledge of persistence is particularly useful for informing appropriate policy responses.

The reduction in water pH may affect a variety of marine organisms, including corals, molluscs and crustaceans, although the magnitude and direction of these effects may vary across species and ecosystems (Lemasson et al., 2017). This causes reef degradation, a decline in fish species, and a reduced capacity of the ocean to absorb CO_2, which exacerbates climate change (Doney et al., 2009; Fabry et al., 2008; Hoegh-Guldberg et al., 2017).

Ocean biogeochemical models project that, under the IPCC, 2000 A2 scenario, the pH of surface water could drop from its pre-industrial value of around 8.2 to approximately 7.8 by the end of the 21st century, which would represent an increase of about 150% in ocean acidity compared to levels at the beginning of the industrial era (Feely et al., 2009). Further, the annual assessment of the Global Carbon Project (Friedlingstein et al., 2025) estimated that global net carbon uptake by the oceans was about 3.0 petagrams of Carbon (PgC) per year, equivalent to about one-quarter of total anthropogenic CO_2 emissions. These data highlight the critical role of oceans as carbon sinks, modulating the increase in atmospheric CO_2 and directly affecting surface water chemistry, including acidification and carbonate availability for calcifying organisms.

Various studies have reported a global average reduction in surface pH in surface pH from the 1980s to the present, with global estimates in the range of –0.06 to –0.08 pH units between 1985 and 2024, and spatial heterogeneity, with regions such as the equatorial Pacific, the Southern Ocean, and parts of the Atlantic, where rates exceed the global average (Lefévre et al., 2016; Chau et al., 2024; Vasanth et al., 2025). These estimates combine *in situ* observations from local stations with hydrographic measurements of both the multidecadal trend and seasonal and interannual variability (Copernicus Marine Environment Monitoring Service, 2024).

Studies at reference stations document detectable changes since the 1990s. The Hawaii Ocean Time-series Station ALOHA series (Lukas et al., 2001) has shown a consistent decline in pH and concomitant increases in CO_2 partial pressure (pCO_2) and dissolved inorganic carbon (DIC), with seasonal structure and variability associated with local physical-biogeochemical processes and the advection of water masses with different chemical histories (Dore et al., 2009; Byrne et al., 2010). Similarly, analyses of hydrographic sections have documented pH decreases at the basin scale and at different depths (Feely et al., 2009; Lefévre et al., 2016).

However, despite the available evidence of a trending behaviour, methodological challenges remain in characterising the evolution over time of ocean pH. Most existing studies run linear regressions of pH on a time trend, carry out slope analysis on annualised series, or perform trend detection tests that control only partially for seasonality and first-order autocorrelation (Dore et al., 2009; Byrne et al., 2010; Feely et al., 2009; Doney et al., 2009). These approaches have been useful to provide evidence of acidification and its ecological implications, but suffer from inherent limitations when the series exhibit more complex dependency structures. For instance, to identify long-term trends in the pH time series of coastal water, Li et al. (2025) used a Generalized Additive Model (GAM), before the Mann-Kendall trend test was applied (Gilbert, 1987). They used the GAM model, which is a generalized linear model containing a sum of smooth, nonparametric functions of covariates (Wood, 2006), in order to remove short term fluctuations before the M-K trend test. This is due to the fact that this test assumes that the data points are not serially correlated over time, but pH exhibits large seasonal and interannual variations. Finally, to calculate the linear trends of the time series, Li et al. (2025) used the non-parametric Theil-Sen estimator (also called Sen's slope estimator) (Wilcox, 2001).

In particular, pH series and the associated variables often exhibit higher-order autocorrelation and long-memory behaviour. The latter property, documented in oceanic and climatic variables such as sea surface temperature or atmospheric CO_2 (Gil-Alana, 2005, 2019, 2024, 2025; Caporale et al., 2025, Martin-Valmayor et al., 2025) implies that the effects of shocks persist for long periods of time, as the adjustment dynamics are slower than those assumed in conventional models based on the dichotomy between I(0) or I (1) series.[1] Therefore, the more recent literature argues in favour of approaches that are more suitable to capture the temporal dependence and persistence in acidification series (Sutton et al., 2022). Specifically, in climate and biogeochemical systems the effects of shocks may disappear very slowly without mean reversion occurring. Consequently, a more general modelling framework should be used. In the context of ocean acidification, a shock refers to any exogenous perturbation affecting the behaviour of the observed series. This may include changes associated with atmospheric CO_2 concentrations, ocean circulation variability, climatic oscillations, volcanic activity, or other environmental disturbances.

Although the Station ALOHA series is widely recognised as one of the most important long-term observational records in ocean acidification research, analysing it should be seen as a benchmark case study rather than as a fully representative description of all oceanic regions. Acidification dynamics may differ substantially across coastal, polar, or upwelling systems due to regional physical and biogeochemical conditions.

For these reasons, the present study applies fractional integration methods to analyse the ocean surface pH time series constructed as part of the Hawaii Ocean Time-series programme at Station ALOHA for the period 1985–2024. It also examines the

1 In brief, an I(0) or integrated of order 0 process is a well-behaved one such that valid statistical inference can be drawn. By contrast, an I(1) process requires first-differencing to make it I(0) and perform valid statistical tests. For this reason, instead of working with the original data y(t), we use their first differences, i.e, y(t) – y(t-1). In an oceanographic (time series) context, a series (like sea level, water temperature or current speed) is stationary I(0) if the mean and variance are constant across time and the covariance between two points in time does not depend on the specific location in time. It must also satisfy the condition that the sum of its autocovariances is finite.

stability of the relevant parameters by using recursive methods with the aim of establishing whether or not the persistence in the series has increased and its downward trends has become more pronounced. The chosen framework, based on fractionally integrated or I(d) processes, allows the order of differentiation d to take any real values, including fractional ones, and can capture a wide range of processes ranging from long-memory stationary (0< d< 0.5) to non-stationary ones with highly persistent shocks (d ≥ 1). Such an approach sheds light on various properties of the data, such as their degree of persistence, mean reversion, the adjustment speed towards the long-run equilibrium, and the transitory or permanent effects of shocks. Previous applications in climate science have demonstrated its ability to describe accurately persistence in temperature series (Gil-Alana, 2005), CO_2 emissions (Belbute and Pereira, 2022), and polar temperatures (Caporale et al., 2025).

The structure of the paper is as follows: Section 2 discusses further the phenomenon of ocean acidification and briefly reviews the relevant literature on this topic; Section 3 outlines the methodology; Section 4 describes the data; Section 5 presents the empirical results; Section 6 offers some concluding remarks.

2 Ocean acidification

Oceans play a crucial role in regulating atmospheric carbon dioxide (CO_2) levels by absorbing large quantities of it (Friedlingstein et al., 2025; Gruber et al., 2023). When CO_2 enters seawater, it dissolves and undergoes chemical reactions that produce bicarbonate ions (HCO_3^-) and protons (H^+). Therefore, it leads to changes in the pH, which is a measure of the concentration of hydrogen ions (H^+), which is calculated as: $pH = -\log_{10}[H^+]$.

Over thousands of years, changes in the ocean pH have been naturally moderated by buffering agents such as carbonate ions (CO_3^{2-}). According to Friedlingstein et al. (2025), the net global uptake of CO_2 by the ocean, called ocean sink, has increased over the years, being equal to 2.9 ± 0.4 gigatonnes of carbon per year (GtC/yr), or (PgC/year), over the period from 2014 to 2023, this representing approximately 26% of total CO_2 emissions. The current pace of CO_2 absorption is too rapid for the natural buffering systems to respond effectively, resulting in substantial alterations to ocean chemistry. These changes include shifts in the concentrations of dissolved CO_2, bicarbonate (HCO_3^-), and carbonate ions (CO_3^{2-}), along with a marked decrease in pH.

The increase of CO_2 oceanic uptake due to anthropogenic CO_2 emissions is commonly referred to as ocean acidification (Caldeira and Wickett, 2003). The International Panel on Climate Change (IPCC, 2011) defined Ocean Acidification as "a reduction in the pH of the ocean over an extended period, typically decades or longer, which is caused primarily by uptake of carbon dioxide from the atmosphere, but can also be caused by other chemical additions or subtractions from the ocean". Hence, it has become a major focus of scientific research over the past two decades due to its potentially severe impact on marine ecosystems and biodiversity (Doney et al., 2009; Dore et al., 2009; Feely et al., 2004; Hoegh-Guldberg et al., 2017; Kroeker et al., 2013; Shinjo et al., 2013; Leung et al., 2022). Since the Industrial Revolution, the average pH of the global surface ocean has decreased by approximately 0.1 units, from 8.2 to 8.1 (Caldeira and Wickett, 2003; Orr et al., 2005; Iida et al., 2021). Jiang et al. (2019) reported a similar global decline of −0.11 ± 0.03 pH units between 1770 and 2000. Most recently, Ma et al. (2023) reported a trend in the global mean pH over the last four decades (1982–2021) of −0.0166 ± 0.0010 per decade. This process is primarily driven by the rising concentration of dissolved inorganic carbon (DIC) in the surface ocean resulting from the uptake of anthropogenic CO_2, although it is partially moderated by fluctuations in naturally occurring DIC.

Several authors have projected a further pH decrease by 2100 in the range of −0.07 to −0.4 units, depending on the future RCP (Representative Concentration Pathway)/SSP (Shared Socioeconomic Pathways) scenarios (Feely et al., 2009; Bopp et al., 2013; Gattuso et al., 2015; Kwiatkowski et al., 2020);. Recently Jiang et al. (2023) reported a projection by the year 2100 of a pH decrease by 0.01, to 8.06 units under SSP 1-1.9, or by 0.39 to 7.68 units under SSP5-8.5, which is even lower than the previously reported value of 7.74 under RCP8.5 based on the GFDL-ESM2M model (Jiang et al., 2019). This difference arises from the different assumptions about land use and energy consumption, which result in higher atmospheric CO_2 projections throughout the 21st century in the SSP scenarios used in CMIP6 compared to the RCP scenarios in CMIP5 (Meinshausen et al., 2011, 2020; Steiner and Reader, 2024). Consequently, this leads to more pronounced surface ocean acidification both globally and regionally (Kwiatkowski et al., 2020; Terhaar et al., 2021). Moreover, according to Hartin et al. (2016) by the year 2300, under a high-emission scenario (RCP 8.5), global surface ocean pH is projected to decline dramatically by 0.77 to 7.50 units.

Most recently, Vasanth et al. (2025) used a multi-variate hybrid machine learning approach to predict future pH trends within the Pacific up to the next century. The analysis revealed a worrying trend: the average pH declines from 7.85 (observed 1973–2021) to 7.84 (predicted 2022–2221). Despite appearing negligible, a 0.01 reduction in pH can have substantial ecological implications, including the alteration of marine food webs and the degradation of the Ocean ecosystem.

Surface warming has been shown to intensify the decline in ocean pH, contributing approximately 15% to the global downward trend (Ma et al., 2023). Therefore, the ongoing decline in seawater's calcium carbonate saturation state, occurring alongside ocean acidification, is expected to hinder the ability of many marine calcifiers to build their calcium carbonate shells and skeletons. This process is projected to have a profound impact on ocean ecosystems over timescales ranging from decades to millennia (Gattuso et al., 2015; Orr et al., 2005; Kwiatkowski et al., 2016, 2020), it has become the focus of many international scientific initiatives (https://www.nanoos.org/) and is one of the targets for SDG14 (https://sdgs.un.org/goals/goal14). However, as already mentioned, a branch of literature shows that studies aimed at monitoring the surface ocean pH and predicting its values in the future have some inherent limitations, as they are typically based on a dichotomy between I(0) and I(1) series which is too restrictive for most hydrological series. Therefore, the present study uses instead a more general fractional integration framework which is more suitable to capture possible trends and persistence in the pH level in the Station ALOHA.

3 Fractional integration

Many hydrological time series display a long memory pattern. Hurst (1951, 1956, 1957) was the first to point out that understanding the long-term variability in the river Nile flow records and other geophysical series required a different modelling approach from previous ones. In the 1960s Mandelbrot and his co-authors defined as the « Hurst effect » the phenomenon occurring when past events have long-lived effects, a property also referred to as long-range dependence or long memory. In particular, Mandelbrot and Van Ness (1968) introduced the process known as fractionaal Brownian motion and showed that fractional Gaussian noise (fGn) could account for those features.

Long memory (LM) can be defined either in the time domain or in the frequency domain. The former definition states that a covariance stationary process $x(t)$[2], $t = 0, \pm 1, \ldots$ with mean μ is LM if the infinite sum of its autocovariances, defined as $\gamma(u) = E[(x(t)-\mu)(x(t+u)- \mu)]$, is infinite, as shown in Equation 1

$$\sum_{u=-\infty}^{u=\infty} |\gamma_u| = \infty\,. \tag{1}$$

Alternatively, the frequency domain definition of LM states that the spectral density function must have at least one pole or singularity in the interval $[0, \pi)$, as shown in Equation 2, as follows:

$$f(\lambda) \to \infty, \quad \text{for } \lambda \quad \text{in } [0, \pi)\,. \tag{2}$$

There are many examples of geophysical series exhibiting these features – see, inter alia, Stephenson et al. (2000), Gil-Alana (2005, 2008, 2017), Vyushin and Kushner (2009), Zhu et al. (2010), Lennartz and Bunde (2009), Rea et al. (2011), Franzke (2010), Yuan et al. (2013, 2022), Zhu et al. (2023) and Gil-Alana and Carmona-González (2024) in a climatological context, and Maftei et al. (2016); Habib (2020), and Niu et al. (2023) in hydrology.

One possible approach to modelling LM processes is based on fractional integration. Specifically, a process is said to be integrated of order d or I(d), where d can be a non-integer value, if it can be expressed as follows in Figure 3:

$$(1 - L)^d x(t) = u(t), \quad t = 0, \pm 1, \ldots, \tag{3}$$

where L is the lag operator, i.e, $L^k x(t) = x(t-k)$, and $u(t)$ is integrated of order 0 or I(0), also known as short memory and characterised by a spectral density function that is positive and bounded at all frequencies. This specification includes white noise as well as weakly autocorrelated processes such as stationary AutoRegressive Moving Averate (ARMA) ones.

If d is positive in Equation 3, x(t) displays the property of long memory since its spectral density function can be formulated as follows in Equation 4:

$$f(\lambda) = \frac{\sigma^2}{2\pi}\left|\frac{1}{1 - e^{i\lambda}}\right|^d, \tag{4}$$

and it tends to infinity as $\lambda \to 0^+$ when $d > 0$. Using a binomial expansion, the L polynomial in (3) can be expressed as follows in Equation 5:

$$\begin{aligned}(1 - L)^d &= \textstyle\sum_{j=0}^{\infty} \binom{d}{j} (-1)^j L^j \\ &= 1 - dL + \frac{d(d-1)}{2} L^2 - \frac{d(d-1)(d-2)}{6} L^3 \ldots,\end{aligned} \tag{5}$$

and thus Equation (3) can be re-written as in Equation 6 as follows:

$$\begin{aligned}x(t) = dx(t-1) - \frac{d(d-1)}{2} x(t-2) + \frac{d(d-1)(d-2)}{6} x(t-3) \\ - \ \ldots \ + \ u(t),\end{aligned} \tag{6}$$

In this context, d measures the degree of dependence (persistence) in the data, with values of d smaller than 1 implying that shocks have transitory effects (i.e., mean reversion occurs), whilst values of d > 1 imply that shocks have permanent effects.

In an oceanographic context, it is important to know the value of d for a given time series as larger values of d indicate that disturbances affecting the pH series tend to persist for longer periods of time and that the system adjusts more slowly to shocks. However, it is worth noting that a high degree of persistence should not be interpreted as evidence of physical irreversibility, but rather as reflecting slow recovery dynamics.

The estimation of the differencing parameter is based on a Lagrange Multiplier test that uses the likelihood function in the frequency domain (Robinson, 1994). This approach allows to build confidence intervals for the values of d at any given significance level, and has been shown to be the most efficient method in the Pitman sense (Pitman, 1949, 1979; Rothe, 1983) against local departures from the null. An issue with this approach is that it is asymptotic (it is a testing procedure with an asymptotical N(0,1) distribution) and the sample size used in the application is very small. We deal with this issue by computing the confidence intervals based on finite sample critical values obtained by means of simulation as in Gil-Alana (2000).[34]

4 Data description

The time series used for the analysis is the Station ALOHA observational record provided by the European Environment

2 2 A covariance stationary process is a process that has a constant mean, a constant variance and a covariance function γ(u) that depends only on the time lag (u), not on the absolute time.

3 3 For each estimation of d (and using different sample sizes in the recursive approach below) we computed critical values based on 10,000 replications in each case. The confidence bands displayed in Figures 2–5 are based on these critical values.

4 The linear structure imposed in Equation 7 might appear as a restrictive assumption. However, when using alternative non-linear models incorporating Chebyshev polynomials in time, the coefficients were statistically insignificant in all cases.

Agency (EEA, 2025). It combines direct pH measurements from the Hawaii Ocean Time-series (HOT) programme at Station ALOHA with gap-filling calculations based on these data (Carter et al., 2016, 2018) as well as a global reconstruction of annual mean surface pH values from CMEMS, obtained from an ensemble of Feed-Forward Neural Networks (Chau et al., 2022) which exploit sampling data gathered in the Surface Ocean CO_2 Atlas (SOCAT database) (Bakker et al., 2016). We use annual data from 1985–2024, with a total of 40 sample observations.

The ALOHA dataset includes *in situ* measurements and pH estimates derived from dissolved inorganic carbon and total alkalinity (Dore et al., 2009). Global mean surface pH values from the Copernicus Marine Service are reconstructed using *in situ* and remote sensing data. This indicator is available annually from 1985 to 2024 (the measurements being taken in January each year, which is in fact a limitation in the sense that seasonal variability is then lost), with individual yearly errors also being provided. The estimated global mean surface seawater pH is based on alkalinity values (obtained using the locally interpolated alkalinity regression (LIAR) method as in Carter et al., 2016, 2018), surface ocean pCO_2 (CMEMS product), and a gridded field of pH values computed from CO_2 system calculations (van Heuven et al., 2011; Copernicus Marine Service, 2021). Further details regarding this ocean monitoring indicator for ocean acidification can be found in section 2.10 of the Ocean State Report 4 (Gehlen et al., 2020). The pH series and the corresponding logged series (both of which are examined below) are plotted in Figure 1; they both exhibit a pronounced downward trend.

Figure A1 in the Appendix shows the correlograms and periodograms of the original and first differenced data. We observe through the correlogram of the original data that the values decay very slowly, consistent with a nonstationary process. Similarly, the periodogram displays the highest value at the lowest frequency. Taking differences, the plots in the lower panel of the figure might indicate stationarity though also evidence that might be consistent with over differentiation.

5 Empirical results

The model used for the empirical investigation includes two deterministic terms, namely a constant and a (linear) time trend. This is standard in the time series literature on unit roots (Bhargava, 1986; Schmidt and Phillips, 1992) and fractional processes (Gil-Alana and Robinson, 1997). The model is specified in Equation 7 as follows:

$$y(t) = \alpha + \beta \ t + x(t), \quad (1 \ -L)^{d} x(t) = u(t), \quad t = 1, \ 2, \ \dots . \quad (7)$$

where α and β are unknown parameters corresponding to the constant and the coefficient on a linear trend respectively, and the I (0) error term is assumed in turn to be a white noise and an autocorrelated process, the latter as in the exponential spectral model of Bloomfield (1973) which approximates AutoRegressive (AR) structures.[3]3 Table 1 displays the coefficient estimates for both the original and the logged data. It can be seen that under the assumption of white noise errors the estimate of d is equal to 0.89 for both series and the time trend coefficient is negative and significant in both cases. Further, the I(1) hypothesis cannot be rejected since d = 1 is within the 95% confidence interval. When

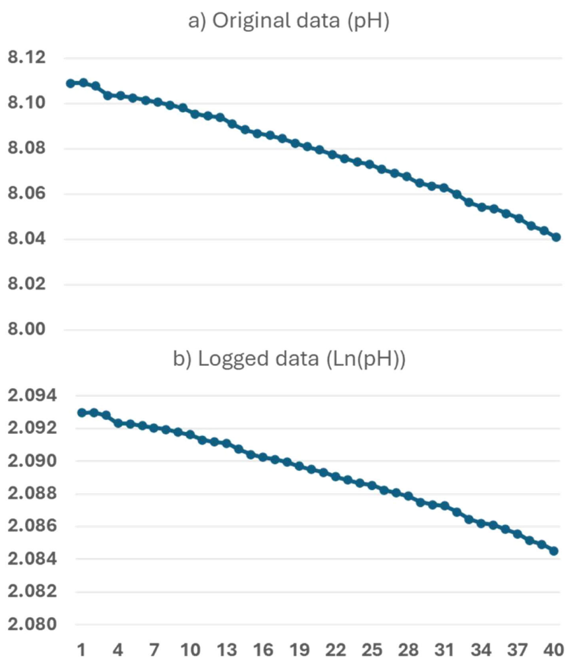

FIGURE 1
Time series plot of **(a)** the original pH data, and **(b)** the Logged pH data. The data are annual and cover the period from 1985 to 2024.

TABLE 1 Estimated coefficients in the model given by Equation 7.

i) White noise errors			
Series	d (95% band)	Intercept (t-stat)	Time trend (t-stat)
Original data	0.89 (0.72, 1.15)	8.11090 (862.41)	-0.00173874 (-16.59)
Logged data	0.89 (0.72, 1.15)	2.09321 (179.35)	-0.00021541 (-16.56)
ii) Autocorrelated (Bloomfield) errors			
Series	d (95% band)	Intercept (t-stat)	Time trend (t-stat)
Original data	0.55 (0.12, 0.96)	8.11222 (103.13)	-0.0017142 (-43.80)
Logged data	0.55 (0.15, 0.97)	2.09337 (214.74)	-0.00021270 (-43.68)

The values in brackets in column 2 and 3 are the t-statistics.

allowing for (weak) autocorrelation, the estimates of d are slightly smaller (0.55), and, in contrast to the previous case, the null hypothesis d = 1 is rejected in favour of mean reversion and shocks with transitory though long-lasting effects. The time trend coefficient is again negative and of the same size as in the white noise case.

The most important feature of the results reported in Table 1 is that the estimates of d are in all cases significantly higher than 0, which supports the null hypothesis of long memory. Specifically, the finding of persistence (indicated by the estimated positive d values) implies that shocks, whether anthropogenic or natural, have long-lived effects. From an oceanographic perspective, this property is consistent with the strong physical and biogeochemical inertia of the surface ocean, where mixing, ventilation, and chemical buffering processes operate on longer timescales than those captured by conventional linear models (Waugh et al., 2006).

Further, the evidence of long memory presented in Table 1 invalidates the estimates based on the assumption of I(0) errors, which is something commonly used in the empirical time series literature and whose results are reported in Table 2 – these erroneously suggest a less pronounced negative trend, namely they underestimate the severity of the acidification phenomenon. This is due to the fact that, by overlooking the inherent persistence of the series, classical methods filter part of the trend signal and interpret it as noise. By contrast, fractional integration methods allow the long-term component to be correctly identified, which explains why the estimated β coefficients are bigger in absolute value when d is allowed to take any real value in the interval (0,1). Thus, the actual decrease in pH, which is crucial to assessing the rate of acidification, is more pronounced than traditional approaches would suggest.

Next we analyse the stability of the coefficients reported in Table 1 by carrying out recursive estimation of both d (persistence) and β (time trend), starting with a sample ending in 2005 and then adding one observation at a time. The results for both the original and the logged data and for both error specifications (white noise and autocorrelation) are displayed in Figures 2–5.

It can be seen that the estimates based on the assumption of white noise errors imply a monotonic increase in d and decrease (increase in absolute value) in β, namely an increasingly high degree of persistence and a more pronounced downward trend in the pH level. For instance, the recursive estimates of the differencing parameter d increase from below 0.4 to above 0.8 over the sample in the case of the original data. While the former implies mean reversion, the latter characterises a situation when shocks have almost permanent effects: a system with a high d responds much more slowly to future reductions in emissions, which means that the pH recovery will take longer even under strict environmental

TABLE 2 Estimated coefficients in the model given by Equation 7 with d = 0.

i) White noise errors			
Series	d (95% band)	Intercept (t-stat)	Time trend (t-stat)
Original data	d = 0	8.11399 (147.87)	-0.0017179 (-73.37)
Logged data	d = 0	2.09359 (303.65)	-0.000210 (-72.53)
ii) Autocorrelated (Bloomfield) errors			
Series	d (95% band)	Intercept (t-stat)	Time trend (t-stat)
Original data	d = 0	8.11399 (265.70)	-0.0017101 (-132.09)
Logged data	d = 0	2.09359 (550.54)	-0.00021208 (-131.53)

The values in brackets in column 2 and 3 are the t-statistics.

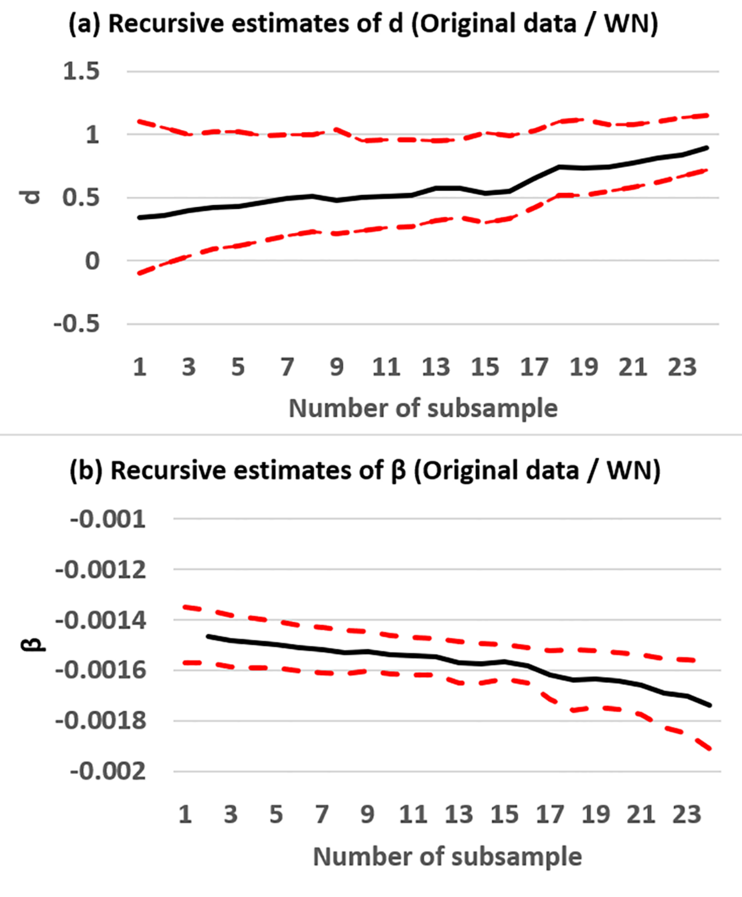

FIGURE 2
Recursive estimates of d and β. Original data and white noise disturbances. The black solid line shows the estimated values of **(a)** d and **(b)** β, whilst the red dash lines display the 95% confidence intervals. The horizontal axis shows the number of subsamples considered starting with the first one ending in 2000 and then adding recursively one observation (year) at a time.

policies. This increase in persistence in recent decades is likely to reflect the sustained rise in CO_2 emissions and the progressive accumulation of anthropogenic carbon in the upper layers of the ocean. Further, the recursive estimates of β, which over the sample period increase in absolute value from around -0.0014 to -0.0017 in the case of the original data, imply that the rate of acidification is accelerating (Hönisch et al., 2012).

Figures 4 and 5 report the corresponding estimates under the assumption of autocorrelated (Bloomfield) errors. These confirm the previous findings, namely they indicate a significant increase in the degree of persistence in both series, the estimated values of d increasing from around -0.5 to above 0.5 in the case of the original series (though mean reversion holds across the sample). Besides, the downward trend in the pH level again appears to have accelerated, especially in the last decade, with the estimated coefficient increasing in absolute value from around -0.0014 to -0.0018 in the case of the original data. The negative values of d observed in the first subsamples are clearly due to numerical instability caused by the small number of observations used in these cases.

A final issue to be addressed is which of the two alternative assumptions about the error term (white noise or autocorrelation) is more appropriate for the data under examination. A direct comparison between the two specifications based on the likelihood function support the uncorrelated approach; however, standard likelihood criteria such as the AIC, BIC might be very sensitive in the context of empirical applications involving fractional differentiation. On the other hand, the fact that the estimates of d are different in the two cases (0.89 with white noise residuals and 0.55 with autocorrelated ones) suggests that allowing for autocorrelation might provide additional information about the memory properties of the series. Further evidence of possible autocorrelation is provided by the plots of the residuals of the detrended and d-differenced processes for both the original and logged data, together with the associated correlograms (see Figure A2 and A3 in Appendix 2). These results might be seen as supporting the hypothesis of autocorrelation in the four series examined. We also computed different ARFIMA(p, d, q) models for all values of p and q smaller or equal to 3, and although these results (not

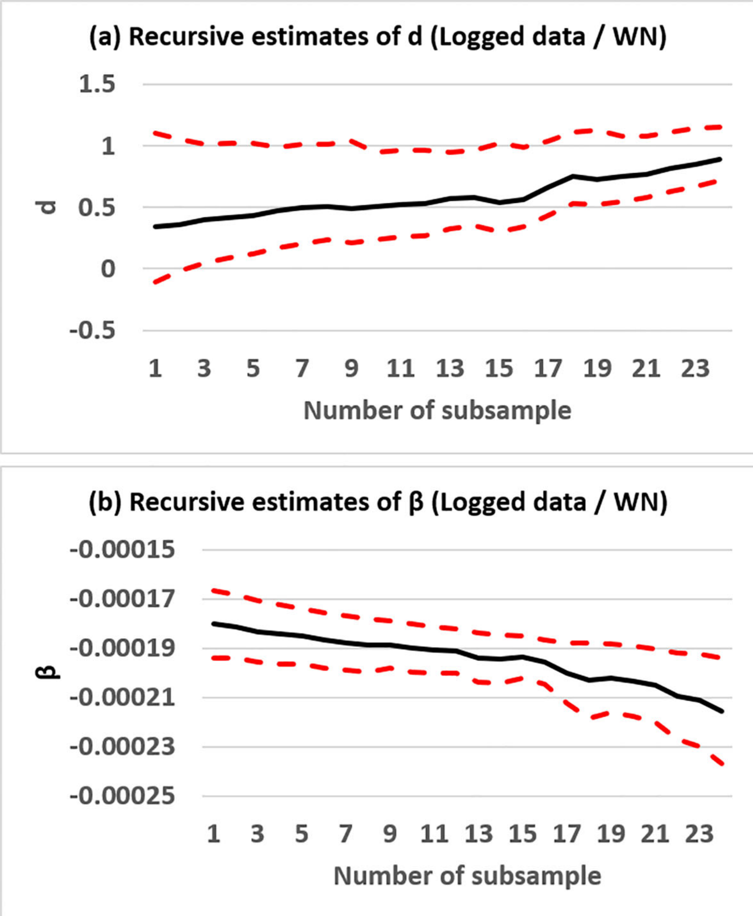

FIGURE 3
Recursive estimates of d and β. Logged data and white noise disturbances. The black solid line shows the estimated values of **(a)** d and **(b)** β, whilst the red dash lines display the 95% confidence intervals. The horizontal axis shows the number of subsamples considered starting with the first one ending in 2000 and then adding recursively one observation (year) at a time.

reported for reasons of space) were sensitive to the choice of these values, all them support the hypothesis of long memory behaviour, which appear to be a robust finding across alternative specifications. While the estimated value of the differencing parameter varies depending on the assumed error structure, all specifications support substantial persistence in the Station ALOHA pH series.

6 Conclusions

In recent decades there has been increasing concern over ocean acidification, namely the observed reduction in the pH level in the Station ALOHA over an extended period of time, whose main cause is the increase in carbon dioxide emissions in the atmosphere resulting from human activities. Several empirical studies have analysed this phenomenon and provided a sizeable a of evidence confirming that the pH level in the oceans has been trending downwards over the years (see, e.g., Caldeira and Wickett, 2003; Orr et al., 2005; Iida et al., 2021; Jiang et al., 2019; Ma et al., 2023). However, some of these studies have used standard econometric models restricting the order of differentiation of the series under examination to integer values.

By contrast, this paper applies fractional integration methods to analyze the decrease in ocean surface pH using the annual Hawaii Ocean Time-series Station ALOHA series for the period 1985–2024. The chosen modelling framework is more general than standard ones based on the I(0) versus I(1) dichotomy and sheds light on the long memory and persistence properties, as well as on the possible presence of trends, in the pH level in Station ALOHA record. The results indicate that the series exhibit a negative and significant time trend; however, whether or not the null hypothesis of a unit root is rejected depends on the assumption made about the errors. The key finding (when the errors are not incorrectly specified as I(0) processes) is the presence of long memory, which implies that the effects of shocks are long-lived, regardless of whether or not mean reversion occurs; in other words, the acidification observed today reflects not only recent emissions, but also a historical legacy that continues to affect the ocean system.

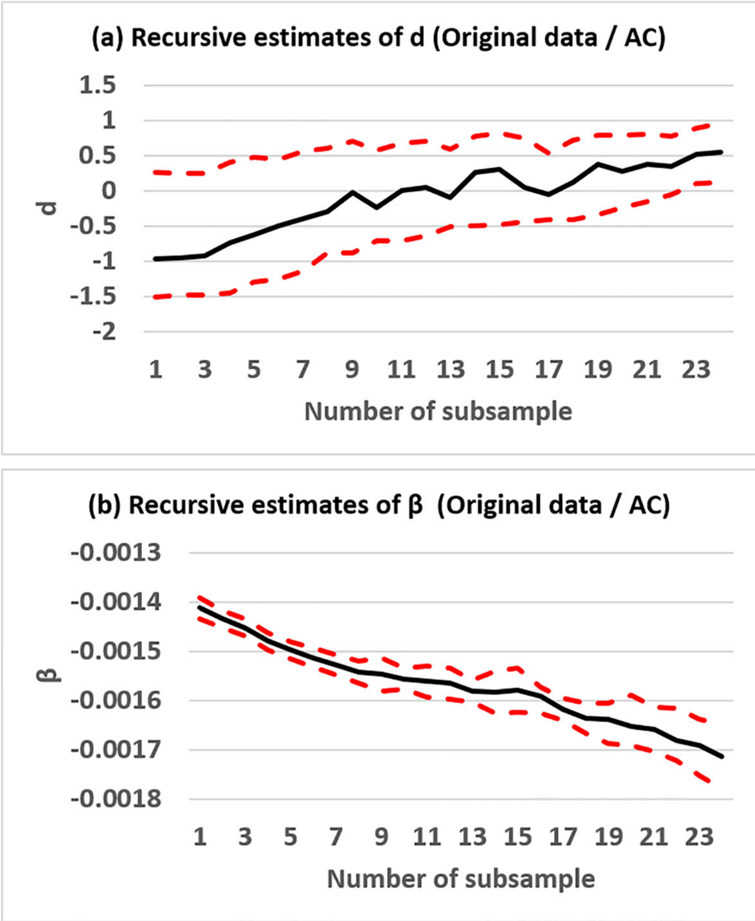

FIGURE 4
Recursive estimates of d and β. Original data and autocorrelated disturbances. The black solid line shows the estimated values of **(a)** d and **(b)** β, whilst the red dash lines display the 95% confidence intervals. The horizontal axis shows the number of subsamples considered starting with the first one ending in 2000 and then adding recursively one observation (year) at a time.

Moreover, the recursive analysis indicates that both the degree of persistence and the downward trend in the pH level have increased over time. This is consistent with oceanographic evidence documenting a progressive increase in anthropogenic CO_2 absorption and an acceleration in acidification in various regional contexts.

These findings reinforce the importance of sustained mitigation efforts and long-term ocean monitoring. The evidence of persistence in the Station ALOHA series suggests that reductions in emissions may take considerable time to be reflected in the evolution of ocean acidification, pointing to slow adjustment dynamics. In this context, the presence of long memory implies that even significant reductions in emissions may not translate into an immediate recovery, but rather into a gradual process over time. Therefore, our results highlight the importance of adopting long-term perspectives when analysing the potential effects of mitigation policies on ocean acidification. However, these results should not be seen as having direct quantitative policy implications, but rather as evidence of persistent dynamics in ocean acidification processes.

Although the results provide clear evidence of persistence in the pH dynamics of the Station ALOHA record, they should be interpreted with caution when considering broader oceanic contexts. The analysis is based on a single long-term observational series widely used as a benchmark in the ocean acidification literature. However, persistence properties may vary across ocean basins due to regional physical and biogeochemical conditions.

In addition, the dataset analysed combines direct observations with reconstructed values obtained through gap-filling and modelling procedures. Although this approach makes it possible to construct a consistent long-term series, it may also introduce additional uncertainty into the analysis, which should be borne in mind when interpreting the results.

Another limitation of the present study is that the analysis focuses exclusively on the statistical properties of the pH series and does not explicitly incorporate potential physical or biogeochemical drivers of ocean acidification. Furthermore, uncertainty associated with the underlying data is not explicitly quantified. Future research

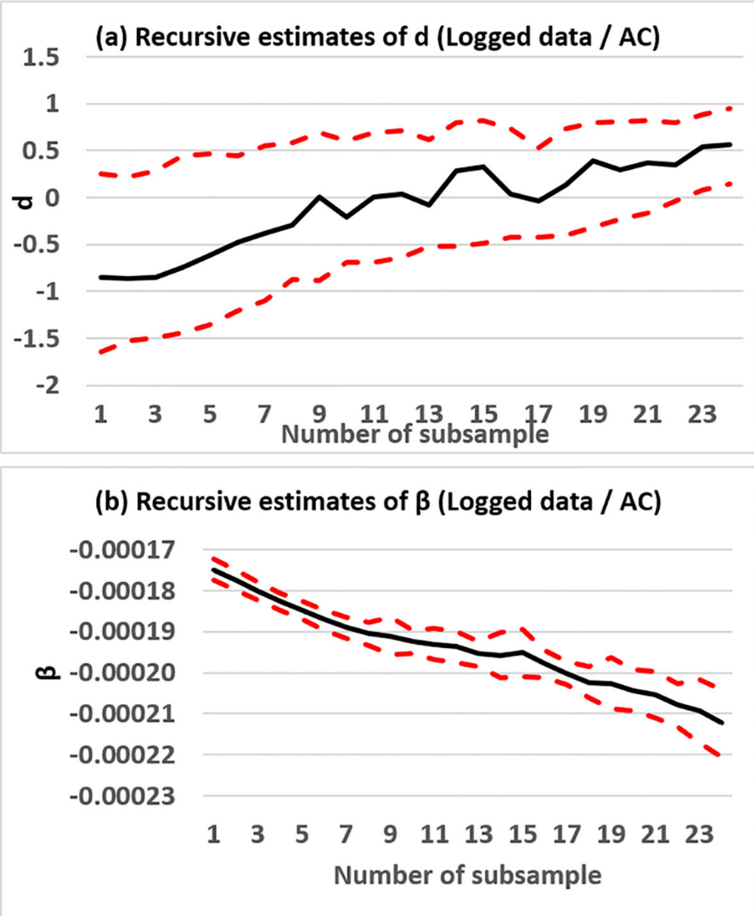

FIGURE 5
Recursive estimates of d and β. Logged data and autocorrelated disturbances. The black solid line shows the estimated values of **(a)** d and **(b)** β, whilst the red dash lines display the 95% confidence intervals. The horizontal axis shows the number of subsamples considered starting with the first one ending in 2000 and then adding recursively one observation (year) at a time.

could address these issues through multivariate approaches and uncertainty propagation techniques.

Future research could extend the fractional integration analysis carried out in the present study to examine additional long-term pH time series from different ocean regions in order to assess the robustness and spatial heterogeneity of long-memory behaviour in ocean acidification processes.

Data availability statement

The datasets analysed in this study are publicly available from the European Environment Agency's ocean acidification indicator. The Station ALOHA pH data originate from the Hawaii Ocean Time-series (HOT) programme, and the annual global mean surface seawater pH data are available through the Copernicus Marine Service.

Author contributions

LG-A: Project administration, Methodology, Writing – review & editing, Investigation, Writing – original draft, Visualization. GC: Formal analysis, Writing – original draft, Investigation, Writing – review & editing, Data curation. NC-G: Supervision, Writing – original draft, Writing – review & editing, Software, Resources. MR-R: Supervision, Writing – original draft, Writing – review & editing, Software, Resources.

Funding

The author(s) declared that financial support was received for this work and/or its publication. All the authors gratefully acknowledge financial support from the project from 'Ministerio de Ciencia, Innovación y Universidades `Agencia Estatal de Investigación' (AEI) Spain and `Fondo Europeo de Desarrollo Regional'

(FEDER), Grant D2023-149516NB-I00 funded by MCIN/AEI/10.13039/501100011033. They also acknowledge support from an internal Project of the Universidad Francisco de Vitoria. He is also grateful for the continuous support of Izaro Gil Cabo.

Acknowledgments

A previous version of this manuscript has been published as CESifo WP no. 12281.

Conflict of interest

The author(s) declared that this work was conducted in the absence of any commercial or financial relationships that could be construed as a potential conflict of interest.

Generative AI statement

The author(s) declared that generative AI was not used in the creation of this manuscript.

Any alternative text (alt text) provided alongside figures in this article has been generated by Frontiers with the support of artificial intelligence and reasonable efforts have been made to ensure accuracy, including review by the authors wherever possible. If you identify any issues, please contact us.

Publisher's note

References

(2023). *Goal 14: Life Below Water*. Available online at: https://www.globalgoals.org/14-life-below-water (Accessed October 23, 2025).

Bakker, D. C. E., Pfeil, B., Landa, C. S., Metzl, N., O'Brien, K. M., Olsen, A., et al. (2016). A multi-decade record of high-quality fCO_2 data in version 3 of the Surface Ocean CO_2 Atlas (SOCAT). *Earth Syst. Sci. Data* 8, 383–413. doi: 10.5194/essd-8-383-2016

Belbute, J. M., and Pereira, A. M. (2022). ARFIMA reference forecasts for worldwide CO_2 emissions and the national dimension of the policy efforts to meet IPCC targets. *J. Econ. Dev.* 47, 1–27. doi: 10.35866/caujed.2022.47.1.001

Bhargava, A. (1986). On the theory of testing for unit roots in observed time series. *Rev. Economic Stud.* 53, 369–384. doi: 10.2307/2297634

Bloomfield, P. (1973). An exponential model in the spectrum of a scalar time series. *Biometrika* 60, 217–226. doi: 10.1093/biomet/60.2.217

Bopp, L., Resplandy, L., Orr, J. C., Doney, S. C., Dunne, J. P., Gehlen, M., et al. (2013). Multiple stressors of ocean ecosystems in the 21st century: projections with CMIP5 models. *Biogeosciences* 10, 6225–6245. doi: 10.5194/bgd-10-3627-2013

Byrne, R. H., Mecking, S., Feely, R. A., and Liu, X. (2010). Direct observations of basin-wide acidification of the North Pacific. *Geophys. Res. Lett.* 37, L02601. doi: 10.1029/2009GL040999

Caldeira, K., and Wickett, M. E. (2003). Oceanography: Anthropogenic carbon and ocean pH. *Nature* 425, 365–365. doi: 10.1038/425365a

Caporale, G. M., Gil-Alana, L. A., and Carmona-González, N. (2025). Some new evidence using fractional integration about trends, breaks and persistence in polar amplification. *Sci. Rep.* 15, 8327. doi: 10.1038/s41598-025-92990-x

Carter, B. R., Feely, R. A., Williams, N. L., Dickson, A., Fong, M. B., and Takeshita, Y. (2018). Updated methods for global locally interpolated estimation of alkalinity, pH, and nitrate. *Limnol. Oceanogr. Methods* 16, 119–131. doi: 10.1002/lom3.10232

Carter, B. R., Williams, N. L., Gray, A. R., and Feely, R. A. (2016). Locally interpolated alkalinity regression for global alkalinity estimation. *Limnol. Oceanogr. Methods* 14, 268–277. doi: 10.1002/lom3.10087

Chau, T. T. T., Gehlen, M., and Chevallier, F. (2022). A seamless ensemble-based reconstruction of surface ocean pCO2 and air–sea CO_2 fluxes over the global coastal and open oceans. *Biogeosciences* 19, 1087–1109. doi: 10.5194/bg-19-1087-2022

Chau, T. T. T., Gehlen, M., Metzl, N., and Chevallier, F. (2024). CMEMS-LSCE: A global, 0.25°, monthly reconstruction of the surface ocean carbonate system. *Earth Syst. Sci. Data* 16, 121–145. doi: 10.5194/essd-16-121-2024

Copernicus Marine Environment Monitoring Service (2024). *Global Ocean Surface Carbon Product: MULTIOBS_GLO_BIO_CARBON_SURFACE_MYNRT_015_008*. Available online at: https://data.marine.copernicus.eu/products (Accessed October 15, 2025).

Copernicus Marine Service (2021). *Global Mean Sea Water Ph*. Available online at: https://marine.copernicus.eu/access-data/ocean-monitoring-indicators/global-mean-sea-water-ph (Accessed October 15, 2025).

Doney, S. C., Fabry, V. J., Feely, R. A., and Kleypas, J. A. (2009). Ocean acidification: The other CO_2 problem. *Ann. Rev. Mar. Sci.* 1, 169–192. doi: 10.1146/annurev.marine.010908.163834

Dore, J. E., Lukas, R., Sadler, D. W., Church, M. J., and Karl, D. M. (2009). Physical and biogeochemical modulation of ocean acidification in the central North Pacific. *Proc. Natl. Acad. Sci.* 106, 12235–12240. doi: 10.1073/pnas.0906044106

European Environmental Agency, EEA (2025). *Ocean Acidification*. Available online at: https://www.eea.europa.eu/en/analysis/indicators/ocean-acidification?activeAccordion=546a7c35-9188-4d23-94ee-005d97c26f2b (Accessed November 8, 2025).

Fabry, V. J., Seibel, B. A., Feely, R. A., and Orr, J. C. (2008). Impacts of ocean acidification on marine fauna and ecosystem processes. *ICES J. Mar. Sci.* 65, 414–432. doi: 10.1093/icesjms/fsn048

Feely, R. A., Doney, S. C., and Cooley, S. R. (2009). Ocean acidification: Present conditions and future changes in a high-CO_2 world. *Oceanography* 22, 36–47. doi: 10.5670/oceanog.2009.95

Feely, R. A., Sabine Lee, C.L. K., Berelson, W., Kleypas, J., and Fabry, V. J. (2004). Impact of anthropogenic CO_2 on the $CaCO_3$ system in the oceans. *Science* 305, 362–366. doi: 10.1126/science.1097329

Franzke, C. (2010). Long-range dependence and climate noise characteristics of Antarctic temperature data. *J. Climate* 23, 6073–6080. doi: 10.1175/2010JCLI3654.1

Friedlingstein, P., O'Sullivan, M., Jones, M. W., Andrew, R. M., Hauck, J., Landschützer, P., et al. (2025). Global carbon budget 2024. *Earth Syst. Sci. Data* 17, 965–1039. doi: 10.5194/essd-17-965-2025

Gattuso, J. P., Magnan, A., Billé, R., Cheung, W. W.L., Howes, E. L., Joos, F., et al. (2015). Contrasting futures for ocean and society from different anthropogenic CO_2 emissions scenarios. *Science* 349, 6243. doi: 10.1126/science.aac4722

Gehlen, M., Chau, T. T.T., Conchon, A., Denvil-Sommer, A., Chevallier, F., Vrac, M., et al. (2020). Ocean acidification. In: Copernicus marine service ocean state report, issue 4. *J. Oper. Oceanogr.* 13, s88–s91. doi: 10.1080/1755876X.2020.1785097

Gil-Alana, L. A. (2000). Evaluation of Robinson's, (1994) tests in finite samples. *J. Stat. Comput. Simul.* 68, 39–63. doi: 10.1080/00949650008812055

Gil-Alana, L. A. (2005). Statistical modeling of the temperatures in the Northern Hemisphere using fractional integration techniques. *J. Clim.* 18, 5357–5370. doi: 10.1175/JCLI3543.1

Gil-Alana, L. A., and Carmona-González, N. (2024). Temperature anomalies in the Northern and Southern Hemispheres: Evidence of persistence and trends. *Adv. Meteorol.* 2024, 8900065. doi: 10.1155/2024/8900065

Gil-Alana, L. A., and Carmona-González, N. (2025). Time trends and persistence in the Arctic temperature. *Meteorol. Atmos. Phys.* 137, 24. doi: 10.1007/s00703-025-01072-0

Gil-Alana, L. A., Monge, M., and Romero-Rojo, M. F. (2019). Sea surface temperatures: Sesonal persistence and trends. *J. Atmos. Ocean. Tech.* 36, 2257–2266. doi: 10.1175/JTECH-D-19-0090.1

Gil-Alana, L. A., and Robinson, P. M. (1997). Testing of unit root and other nonstationary hypotheses in macroeconomic time series. *J. Econometrics* 80, 241–268. doi: 10.1016/S0304-4076(97)00038-9

Gil-Alana, L. A. (2008). Time trend estimation with breaks in temperature time series. *Climatic Change* 89, 325–337. doi: 10.1007/s10584-008-9407-z

Gil-Alana, L. A. (2017). Alternative modelling approaches for the ENSO time series: persistence and seasonality. *Int. J. Climatol.* 37, 2354–2363. doi: 10.1002/joc.4850

Gilbert, R. O. (1987). *Statistical Methods for Environmental Pollution Monitoring* (New York, USA: Wiley).

Gruber, N., Bakker, D. C.E., DeVries, T., Gregor, L., Hauck, J., Landschützer, P., et al. (2023). Trends and variability in the ocean carbon sink. *Nat. Rev. Earth Environ.* 4, 119–134. doi: 10.1038/s43017-022-00381-x

Habib, A. (2020). Exploring the physical interpretation of long-term memory in hydrology. *Stoch. Environ. Res. Risk Assess.* 34, 2083–2091. doi: 10.1007/s00477-020-01883-0

Hartin, C. A., Bond-Lamberty, B., Patel, P., and Mundra, A. (2016). Ocean acidification over the next three centuries using a simple global climate carbon-cycle model: projections and sensitivities. *Biogeosciences* 13, 4329–4342. doi: 10.5194/bg-13-4329-2016

Hoegh-Guldberg, O., Poloczanska, E. S., Skirving, W., and Dove, S. (2017). Coral reef ecosystems under climate change and ocean acidification. *Front. Mar. Sci.* 4, 158. doi: 10.3389/fmars.2017.00158

Hönisch, B., Ridgwell, A., Schmidt, D. N., Thomas, E., Gibbs, S. J., Sluijs, A., et al. (2012). The geological record of ocean acidification. *Science* 335, 1058–1063. doi: 10.1126/science.1208277

Hurst, H. E. (1951). Long-term storage capacity of reservoirs. *Trans. Am. Soc Civ. Eng.* 116, 770–808. doi: 10.1061/TACEAT.0006518

Hurst, H. E. (1956). Methods of using long-term storage in reservoirs. *Proc. Inst. Civ. Eng.* 5, 519–543. doi: 10.1680/iicep.1956.11503

Hurst, H. E. (1957). A suggested statistical model of some time series which occur in nature. *Nature* 180, 494. doi: 10.1038/180494a0

Iida, Y., Takatani, Y., Kojima, A., and Ishii, M. (2021). Global trends of ocean CO_2 sink and ocean acidification: an observation-based reconstruction of surface ocean inorganic carbon variables. *J. Oceanogr.* 77, 323–358. doi: 10.1007/s10872-020-00571-5

IPCC (2000). *Special Report on Emissions Scenarios (SRES): A Special Report of Working Group III of the Intergovernmental Panel on Climate Change* (Cambridge University Press). Available online at: https://www.ipcc.ch/report/emissions-scenarios/ (Accessed October 23, 2025).

IPCC (2011). *Workshop on Impacts of Ocean Acidification on Marine Biology and Ecosystems. , Japan 17-19 January 2011*. Available online at: https://archive.ipcc.ch/pdf/supporting-material/IPCC_IAOMBE_WorkshopReport_Japan.pdf (Accessed October 23, 2025).

Jiang, L. Q., Carter, B. R., Feely, R. A., Lauvset, S. K., and Olsen, A. (2019). Surface ocean pH and buffer capacity: past, present and future. *Sci. Rep.* 9, 18624. doi: 10.1038/s41598-019-55039-4

Jiang, L.-Q., Dunne, J., Carter, B. R., Tjiputra, J. F., Terhaar, J., Sharp, J. D., et al. (2023). Global surface ocean acidification indicators from 1750 to 2100. *J. Adv. Model. Earth Syst.* 15, e2022MS003563. doi: 10.1029/2022MS003563

Kroeker, K. J., Kordas, R. L., Crim, R., Hendriks, I. E., Ramajo, L., Singh, G. S., et al. (2013). Impacts of ocean acidification on marine organisms: Quantifying sensitivities and interaction with warming. *Glob. Change Biol.* 19, 1884–1896. doi: 10.1111/gcb.12179

Kwiatkowski, L., Gaylord, B., Hill, T., Hosfelt, J., Kroeker, K. J., Nebuchina, Y., et al. (2016). Nighttime dissolution in a temperate coastal ocean ecosystem increases under acidification. *Sci. Rep.* 6, 22984. doi: 10.1038/srep22984

Kwiatkowski, L., Torres, O., Bopp, L., Aumont, O., Chamberlain, M., Christian, J. R., et al. (2020). Twenty-first century ocean warming, acidification, deoxygenation, and upper-ocean nutrient and primary production decline from CMIP6 model projections. *Biogeosciences* 17, 3439–3470. doi: 10.5194/bg-17-3439-2020

Lefévre, N., Veleda, D., Araujo, M., and Caniaux, G. (2016). Variability and trends of carbon parameters at a time series in the eastern tropical Atlantic. *Tellus B. Chem. Phys. Meteorol.* 68, 30305. doi: 10.3402/tellusb.v68.30305

Lemasson, A. J., Fletcher, S., Hall-Spencer, J. M., and Knights, A. M. (2017). Linking the biological impacts of ocean acidification on oysters to changes in ecosystem services: a review. *J. Exp. Mar. Biol. Ecol.* 492, 49–62. doi: 10.1016/j.jembe.2017.01.019

Lennartz, S., and Bunde, A. (2009). Trend evaluation in records with long-term memory: Application to global warming. *Geophys. Res. Lett.* 36, L16706. doi: 10.1029/2009GL039516

Leung, J. Y. S., Zhang, S., and Connell, S. D. (2022). Is Ocean Acidification Really a Threat to Marine Calcifiers? A Systematic Review and Meta-Analysis of 980+ Studies Spanning Two Decades. *Small* 18, 2107407. doi: 10.1002/smll.202107407

Li, M., Li, R., Guo, Y., Testa, J. M., Cai, W.-J., Shen, C., et al. (2025). Disentangling the effects of global and regional drivers on diverse long-term pH trends in coastal waters. *AGU Adv.* 6, e2024AV001350. doi: 10.1029/2024AV001350

Lukas, R., Church, M. J., and Karl, D. M. (2001). "Physical and biochemical oceanographic data from the Hawaii Ocean Time-series (HOT) program collected by University of Hawaii at Station ALOHA in the Pacific Ocean 100 miles north of Oahu, Hawaii, since 1988," in *NOAA National Centers for Environmental Information*. Asheville, United States: NOAA NAtional Centers for Environmental Information. Available online at: https://www.ncei.noaa.gov/archive/accession/Station-ALOHA-HOT (Accessed October 12, 2025).

Ma, D., Gregor, L., and Gruber, N. (2023). Four decades of trends and drivers of global surface ocean acidification. *Global Biogeochem. Cycles* 37, e2023GB007765. doi: 10.1029/2023GB007765

Maftei, C., Barbulescu, A., and Carsteanu, A. A. (2016). Long-range dependence in the time series of Taiţa River discharges. *Hydrolog. Sci. J.* 61, 9. doi: 10.1080/02626667.2016.1171869

Mandelbrot, B. B., and Van Ness, J. W. (1968). Fractional Brownian motions, fractional noises and applications. *SIAM Rev.* 10, 422–437. doi: 10.1137/1010093

Martin-Valmayor, M. A., Infante, J., Carmona-González, N., and Gil-Alana, L. A. (2025). US CO_2 emissions and IPCC components: Evidence of persistence using fractional integration. *Environ. Sustain. Indic.* 26, 100684. doi: 10.1016/j.indic.2025.100684

Meinshausen, M., Smith, S. J., Calvin, K., Daniel, J. S., Kainuma, M. L.T., Lamarque, J.-F., et al. (2011). The RCP greenhouse gas concentrations and their extensions from 1765 to 2300. *Clim. Change* 109, 213–241. doi: 10.1007/s10584-011-0156-z

Meinshausen, M., Nicholls, Z. R.J., Lewis, J., Gidden, M. J., Vogel, E., Freund, M., et al. (2020). The shared socioeconomic pathway (SSP) greenhouse gas concentrations and their extensions to 2500. *Geosci. Model. Dev.* 13, 3571–3605. doi: 10.5194/gmd-13-3571-2020

Niu, J., Xie, P., Sang, Y.-F., Zhang, L., Wu, L., Zhu, Y., et al. (2023). Quantification of long-range dependence in hydroclimatic time series: a method-comparison study. *J. Appl. Meteorol. Climatol.* 62, 1921–1942. doi: 10.1175/JAMC-D-23-0129.1

Orr, J. C., Fabry, V. J., Aumont, O., Bopp, L., Doney, S. C., Feely, R. A., et al. (2005). Anthropogenic ocean acidification over the twenty-first century and its impact on calcifying organisms. *Nature* 437, 681–686. doi: 10.1038/nature04095

Pitman, E. J. G. (1949). Notes on nonparametric statistical inference. New York.

Pitman, E. J. G. (1979). *Some Basic Theory for Statistical Inference* (London: Chapman and Hall).

Rea, W., Reale, M., and Brown, J. (2011). Long memory in temperature reconstructions. *Climatic Change* 107, 247–265. doi: 10.1007/s10584-011-0068-y

Robinson, P. M. (1994). Efficient tests of nonstationary hypotheses. *J. Amer. Statist. Assoc.* 89, 1420–1437. doi: 10.1080/01621459.1994.10476880

Rothe, G. (1983). Some properties of the asymptotic relative Pitman efficiency. *Ann. Stat.* 9, 663–669. doi: 10.1214/AOS/1176345470

Schmidt, P., and Phillips, P. C. B. (1992). LM tests for a unit root in the presence of deterministic trends. *Oxford Bull. Econ Stat* 54, 257–287. doi: 10.1111/j.1468-0084.1992.tb00002.x

Shinjo, R., Asami, R., Huang, K.-F., You, C.-F., and Iryu, Y. (2013). Ocean acidification trend in the tropical North Pacific since the mid-20th century reconstructed from a coral archive. *Mar. Geol.* 342, 58–64. doi: 10.1016/j.margeo.2013.06.002

Steiner, N. S., and Reader, C. M. (2024). Trends and projections in climate-related stressors impacting Arctic marine ecosystems—a CMIP6 model analysis. *J. Geophys. Res. Oceans* 129, e2024JC020970. doi: 10.1029/2024JC020970

Stephenson, D. B., Pavan, V., and Bojariu, R. (2000). Is the North Atlantic Oscillation a random walk? *Int. J. Climatol.* 20, 1–18. doi: 10.1002/(SICI)1097-0088(200001)20:1<1::AID-JOC456>3.0.CO;2-P

Sutton, A. J., Battisti, R., Carter, B., Evans, W., Newton, J., Alin, S., et al. (2022). Advancing best practices for assessing trends of ocean acidification time series. *Front. Mar. Sci.* 9, 1045667. doi: 10.3389/fmars.2022.1045667

Terhaar, J., Torres, O., Bourgeois, T., and Kwiatkowski, L. (2021). Arctic Ocean acidification over the 21st century co-driven by anthropogenic carbon increases and freshening in the CMIP6 model ensemble. *Biogeosciences* 18, 2221–2240. doi: 10.5194/bg-18-2221-2021

United Nations (2025). *Measuring Progress Special Edition, Disaggregation*. Available online at: https://sdgs.unep.org/article/sdg-indicator-1431?utm_source=chatgpt.com (Accessed October 15, 2025).

van Heuven, S., Pierrot, D., and Wallace, D. (2011). CO2SYS v 1.1: MATLAB program developed for CO2 system calculations. ORNL/CDIAC-105b, Carbon Dioxide Information Analysis Center, Oak Ridge National Laboratory, US Department of Energy, Oak Ridge, TN.

Vasanth, K., Kishore, R. K., Sugumaran, V., Krishnamoorthy, R., Ramdas, R., and Tadepalli, S. K. (2025). Multi-variate hybrid modeling for pacific ocean acidification: predicting future pH trends and analyzing key biogeochemical drivers. *CSIT* 13, 99–116. doi: 10.1007/s40012-024-00406-4

Vyushin, D. I., and Kushner, P. J. (2009). Power-Law and Long-Memory Characteristics of the Atmospheric General Circulation. *Journal of Climate* 22, 2890–2904. doi: 10.1175/2008JCLI2528.1

Waugh, D. W., Hall, T. M., McNeil, B. I., Key, R., and Matear, R. J. (2006). Anthropogenic CO_2 in the oceans estimated using transit time distributions. *Tellus B. Chem. Phys. Meteorol.* 58, 376–389. doi: 10.1111/j.1600-0889.2006.00222.x

Wilcox, R. R. (2001). *Fundamentals of Modern Statistical Methods: Substantially Improving Power and Accuracy* (New York, USA: Springer-Verlag).

Wood, S. A. (2006). *Generalized Additive Models: An Introduction With R* (USA: CRC Press). doi: 10.1201/9781315370279

Yuan, N., Fu, Z., and Liu, S. (2013). Long-term memory in climate variability: A new look based on fractional integral techniques. *J. Geophys. Res. Atmos.* 118, 12962–12969. doi: 10.1002/2013JD020776

Yuan, N., Franzke, C. L. E., Xiong, F., Fu, Z., and Dong, W. (2022). The impact of long-term memory on the climate response to greenhouse gas emissions. *npj Clim. Atmos. Sci.* 5, 70. doi: 10.1038/s41612-022-00298-8

Zhu, X., Fraedrich, K., Liu, Z., and Blender, R. (2010). A demonstration of long term memory and climate predictability. *J. Clim.* 23, 5021–5029. doi: 10.1175/2010JCLI3370.1

Zhu, J., Xie, A., Qin, X., Xu, B., and Wang, Y. (2023). Assessment of Antarctic Amplification Based on a Reconstruction of Near-Surface Air Temperature. *Atmosphere* 14, 218. doi: 10.3390/atmos14020218

Appendix

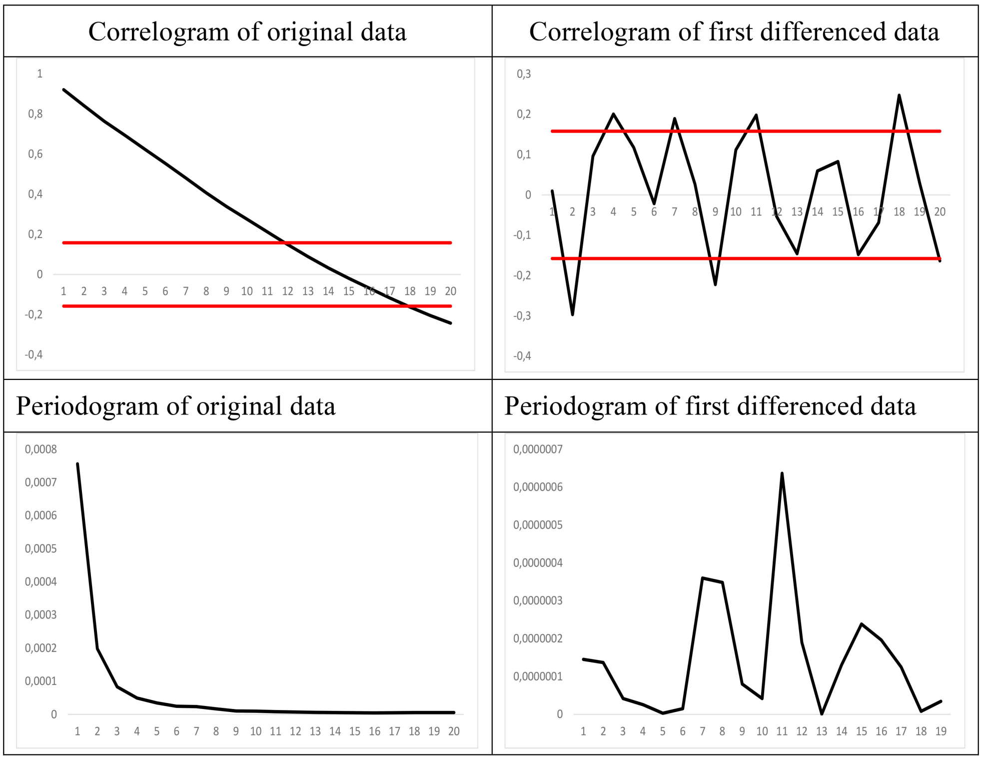

FIGURE A1
Correlograms and periodograms of the original and first differenceddata.

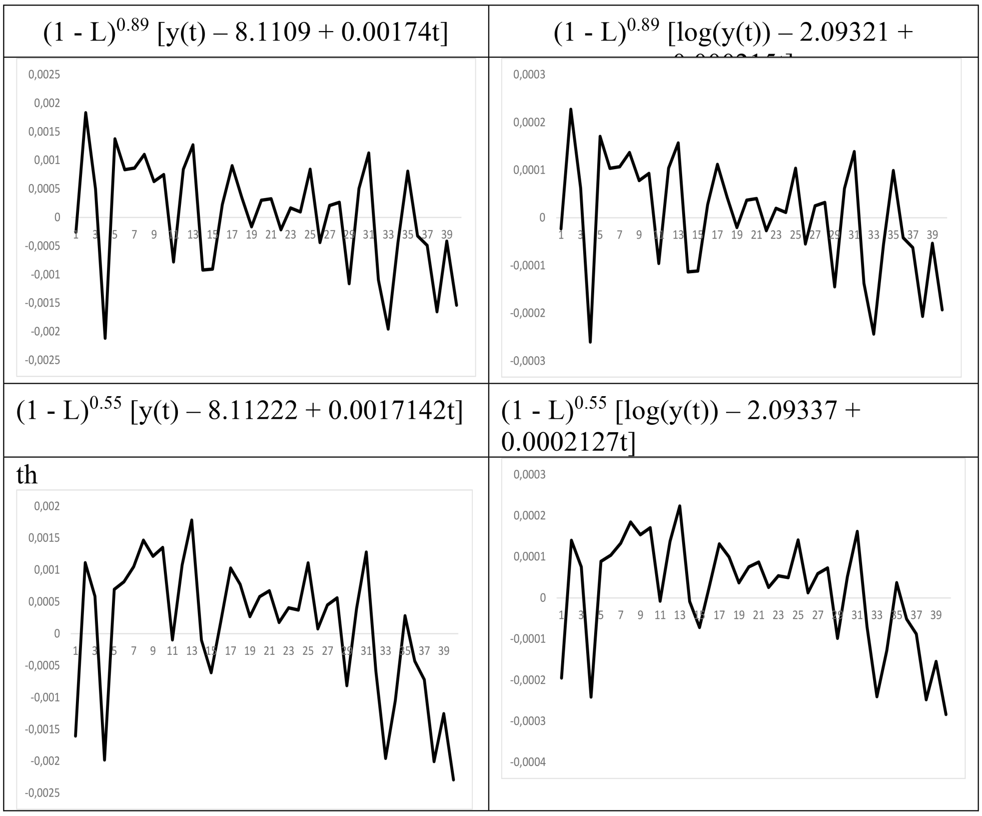

FIGURE A2
Time series plots of the d-differenced detrended series. The series in the left and right panels are based on the original and logged data respectively. The upper panels show the residuals of the detrended series once they are 0.89-differenced, whilst the lower panels plot the 0.55-differenced ones.

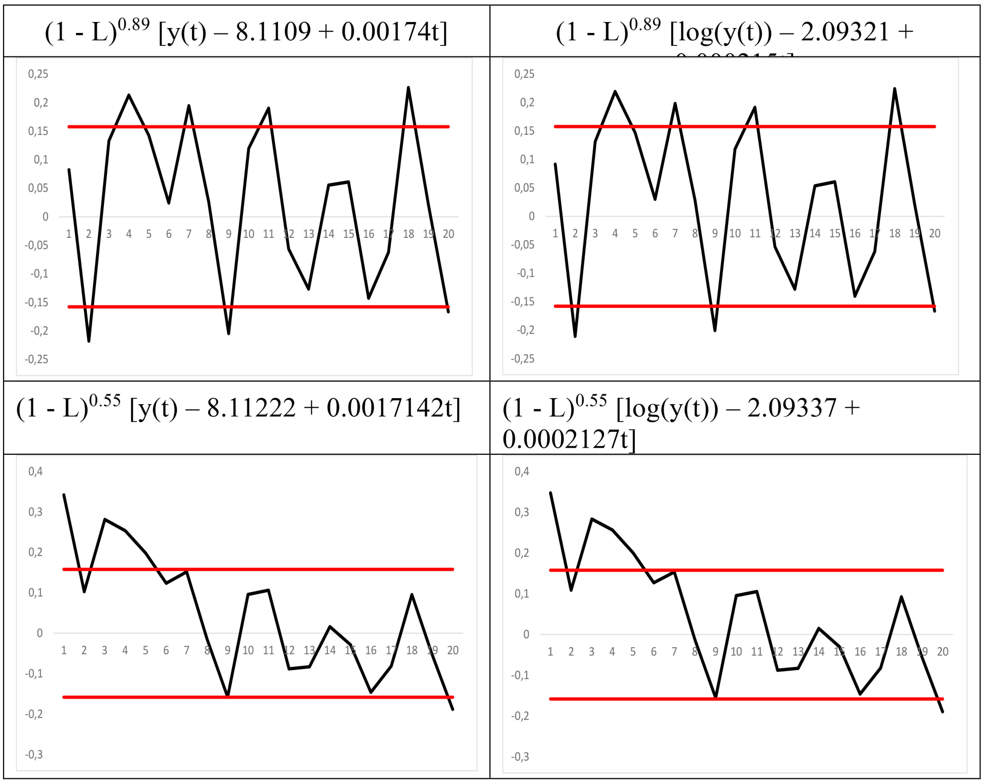

FIGURE A3
Correlograms of the d-differenced detrended series. The series in the left and right panels are based on the original and logged data respectively. The confidence bands correspond to (-1.96/√T,1.96/√T).